

RSC Advances



This is an *Accepted Manuscript*, which has been through the Royal Society of Chemistry peer review process and has been accepted for publication.

Accepted Manuscripts are published online shortly after acceptance, before technical editing, formatting and proof reading. Using this free service, authors can make their results available to the community, in citable form, before we publish the edited article. This *Accepted Manuscript* will be replaced by the edited, formatted and paginated article as soon as this is available.

You can find more information about *Accepted Manuscripts* in the [Information for Authors](#).

Please note that technical editing may introduce minor changes to the text and/or graphics, which may alter content. The journal's standard [Terms & Conditions](#) and the [Ethical guidelines](#) still apply. In no event shall the Royal Society of Chemistry be held responsible for any errors or omissions in this *Accepted Manuscript* or any consequences arising from the use of any information it contains.

MS ID: RA-ART-04-2014-003717 - Revised

Prebiotic synthesis of triazines from urea: A theoretical study of free radical routes to melamine, ammeline, ammelide and cyanuric acid

Yassin A. Jeilani,^{*,a} Thomas M. Orlando,^{*,b} Albryona Pope,^a Claire Pirim,^b Minh Tho Nguyen^{*,c}

^{a)} Department Chemistry and Biochemistry, Spelman College, Atlanta, GA 30314, USA

^{b)} School of Chemistry and Biochemistry, Georgia Institute of Technology, Atlanta, GA 30332, USA

^{c)} Department of Chemistry, University of Leuven, B-3001 Leuven, Belgium

(Abstract)

Prebiotic formation of triazines from urea was studied using density functional theory methods with the aim of understanding some of the neutral precursors that can lead to a mixture of triazines. The proposed mechanisms are based on free radical routes without solvent requirements that are appropriate for prebiotic scenarios occurring under highly non-equilibrium conditions. These include spark discharge or ultraviolet driven reactions taking place on or within low temperature ice or reactions simulated by meteoritic impact on organic surfaces on Titan and possibly early Earth. The ice increases radical lifetimes while the impact events produce sufficient heat to generate useful free radical densities in the impact zones. The mechanisms proceed through relatively small energy barriers. The pathways predict that biuret is a precursor for cyanuric acid, and guanylurea is a

precursor for both melamine and ammeline. Based on the predicted precursors of the triazines, the established mechanisms provide a theoretical support for previous thermal synthesis of the triazines from urea and biuret.

Keywords: triazines, free radicals, prebiotic molecules, urea, density functional theory

*) E-mails: yjeilani@spelman.edu, minh.nguyen@chem.kuleuven.be, and thomas.orlando@chemistry.gatech.edu

I. Introduction

Melamine, ammeline, ammelide, and cyanuric acid belong to the 1,3,5-triazine family of organic compounds. Triazines have been formed in prebiotic simulation experiments and have been detected within complex mixtures of C- and N-bearing compounds. These complicated mixtures are often collectively referred to as tholins.^{1,2} Several experiments have suggested that tholins or tholin-like materials are also likely involved in the formation of organic aerosols in the haze layer in Titan's atmosphere. Indeed, tholins possessing similar optical properties to those observed on Titan, Saturn's largest moon, have been shown to contain triazines.^{1,2}

Also, it appears that Fischer-Tropsch reactions may have been a source of organic compounds in meteorites.³ Melamine, ammeline, and cyanuric acid have been identified in meteoritic samples. Melamine, cyanuric acid, guanylurea and urea were also identified in the Murchison C2 chondrite samples after acid hydrolysis.⁴ There is also evidence that suggests triazines could be formed by processes that may have occurred in the solar nebula.² However, the origin of the organic and nitrogen containing matter in carbonaceous chondrites and in the solar nebula is still not well established and requires further mechanistic investigations.

In laboratory experiments, triazines can be formed from a mixture of simple gases or directly from urea as the only source of C and N. Hayatsu *et al.* reported formation of melamine, ammeline, and cyanuric acid spontaneously from CO, H₂, and NH₃ mixture.⁵ Also urea and biuret were detected in these experiments.⁵ Most probably urea and biuret

are formed first and then consumed as precursors for the triazines. Formation of triazines from urea/ice mixture was recently reported⁶ but this required spark discharge activation. In addition, Briggs et al. reported formation of urea in the photolysis of CO, NH₃, and H₂O mixture at a low temperature of 12 K.⁷ These studies further support the idea that urea could have been an important source of triazines and other organic compounds. Both urea and biuret have also been suggested as prebiotic purine precursors.⁸

In addition, triazines such as cyanuric acid have unique structural features that lead to the formation of supramolecular assemblies by non-covalent interactions. These non-covalent interactions may have played a role in prebiotic chemistry, with unique physicochemical properties in non-terrestrial environments. The symmetry and the multiple functional groups of triazines make them good monomer candidates for self-assemblies. Indeed, Cafferty *et al.* demonstrated that cyanuric acid together with functionalized-pyrimidines yields supramolecular polymer assemblies, thus, providing new ways to make RNA-like polymers.⁹ Such a supramolecular self-assembly has been previously considered under prebiotic conditions.¹⁰ Melamine was also demonstrated to form hydrogen-bonded supramolecular structures with N-heterocycles.¹¹ The possible role of melamine and cyanuric acid in self-assembly processes provides new insight in prebiotic chemistry.

The current project describes mechanisms for the formation of melamine, ammeline, ammelide, and cyanuric acid from urea. The mechanisms are consistent with a recent study for the synthesis of the triazines when urea was subjected to freeze-thaw cycles and spark discharges under CH₄/N₂/H₂ or argon atmosphere.⁶ The mechanisms are

based on the fact that both biuret ($\text{NH}_2\text{CONHCONH}_2$) and guanylurea ($\text{NH}_2\text{CONHCNHNH}_2$) are condensation products of two urea molecules and are precursors of cyanuric acid and melamine/ammeline, respectively. The use of spark discharges for the formation of triazines suggests that free radicals may be involved in the processes. Electron spin resonance spectroscopy analysis of tholins produced by spark discharges showed both carbon-centered and nitrogen-centered free radicals¹² and carbon-carbon bond forming free radical reactions were previously suggested to take place at low temperature. Bernstein *et al.* proposed that these carbon-carbon bonds may be formed by the reaction of either “hot” radicals generated by photolysis at 12 K or “cold” radicals mobilized by an increase in temperature.¹³ Therefore, the current study focuses on the density functional theory calculations for the formation of triazines by free radical pathways. We previously reported free radical pathways to describe the potential prebiotic synthesis of a mixture of nucleobases from formamide.^{14, 15} Our strategy has been finding of mechanisms that lead to a mixture of a group of related compounds. Such strategies are consistent with experimental observations of formation of a mixture of products. The current study focuses on the formation of triazines from urea by free radical pathways making use of quantum chemical computations with density functional theory (DFT). These reactions can occur both in the gas-phase and condensed-phase providing non-thermal excitation sources are available.

II. Computational Methods

All standard calculations using density functional theory (DFT) were performed with the aid of the Gaussian 09 suite of programs.¹⁶ The hybrid B3LYP functional,^{17, 18} in conjunction with the 6-311G(d,p) basis set¹⁹ was used for all calculations. Harmonic vibrational frequency calculations were carried out at the same level in order to confirm the nature of stationary points, and to obtain zero-point vibrational energies. Each transition structure was characterized by having one imaginary vibrational frequency for the normal mode corresponding to the correct reaction coordinate. Geometrical parameters of the relevant stationary points are listed in the Supplementary Information (ESI) file. Our recent theoretical studies^{20,21} pointed out that the B3LYP functional is suitable for investigating reaction pathways involving formamide. The use of this DFT method, in the unrestricted formalism (UB3LYP), allows us to study open-shell radicals.²²⁻²⁴

III. Results and Discussions

In order to facilitate the reading, Figure 1 shows the structures of the triazines investigated here. Both theoretical and experimental work over the past decades on triazines led to the development of scenarios that could lead to the formation of triazines in prebiotic plausible conditions. Because of the structural similarities of the selected four triazines (Figure 1), experiments have shown that urea could be the main source of C and N. The mechanisms described here are based on the formation of the triazines in spark discharge experiments when urea: water ice mixtures was subjected to freeze-thaw cycles under argon.⁶ Under such experimental conditions, free radical mechanisms are likely to

occur. In fact, ice has been suggested as a good gettering source of free radicals for heterocycles.²⁵ Experimental evidence indicating biuret as a precursor for triazines can also now be addressed using the free radical mechanism. Table 1 shows the changes in energies of the pathways leading to the formation of triazines from urea.

1. Validation of the DFT methods

To test the effect of basis set on the energetics along the routes, the structures optimized at B3LYP/6-311G(d,p) level of theory in Scheme 1 were thus subjected to geometry re-optimizations using a large basis set 6-311++(3df, 3pd). Figure 2 shows that the results from the larger B3LYP/6-311++(3df, 3pd) +ZPE energies are comparable to those obtained using the smaller 6-311G(d,p) basis set. The overall pattern of the barrier heights is not changed. These results suggest that the transition state is not substantially affected by the size of the basis set, and similarly the minimum energy paths.

In addition, our DFT methods were compared with CCSD(T) computations. The computations using CCSD(T) methods require enormous computer time with our current computer hardware for the species involved along the pathways, therefore, only the first step of the mechanism was tested. The computation of the first step of the mechanism (**1** → **2**) using CCSD(T)/6-311G(d,p) gave a change of energy of 2.1 kcal/mol that is comparable to the value of -0.3 kcal/mol (Table 1) calculated at B3LYP/6-311G(d,p). Similar differences in energy of less than 2.5 kcal/mol between the two methods was previously reported.²⁰ This validation suggests that the calculations performed at B3LYP/6-311G(d,p) in the present study are reasonably accurate.

2. Mechanisms for the Formation of Melamine

Formation of melamine likely requires three molecules of urea (Scheme 1). The energy profile schematically illustrating the process is summarized in Figure 2. Only the lowest-lying pathway is shown. Let us now describe the steps in some detail. The first step is an activation of urea to generate the radical intermediate **2**. The energy barrier for urea activation is relatively small and is calculated to be 4.8 kcal/mol (Figure 2). In the current mechanism, three sequential steps have been further identified to lead to the formation of guanylurea (**5**). The first step is the radical addition of **2** to the carbonyl group of urea that proceeds through an energy barrier of 19.0 kcal/mol. This is followed by a 1,3-H-rearrangement from N to O (**3** \rightarrow **4**). This 1,3-H rearrangement proceeds through a four-membered ring transition state with an energy barrier of 22.4 kcal/mol (Figure 2). The energy profile suggests that this reaction is reversible with relatively no change in net energy (Table 1). The reversibility of this type of reaction is important because the oxygen radical in **3** may lead to an elimination of a $\bullet\text{NH}_2$ radical as an alternate route. We will see later that the elimination of $\bullet\text{NH}_2$ is important for the route leading to cyanuric acid. The 1,3-H rearrangement is then followed by a radical induced elimination of an $\bullet\text{OH}$ leading eventually to the formation of guanylurea (**5**). Of note, guanylurea (**5**) in Scheme 1 has been previously described as the condensation product of urea. Thus, because steps 3 and 4 may lead to the formation of $\bullet\text{NH}_2$ or $\bullet\text{OH}$, one may also consider that they could be involved in a H-abstraction reaction from urea to generate more of **2**.

The carbonyl group in guanylurea (**5**) is susceptible to a radical attack by **2**. Addition of **2** to guanylurea (**5**) provides the last C needed for melamine. The energy

barrier for **5** \rightarrow **6** step is evaluated to be 20.6 kcal/mol (Figure 2). As expected, this energy barrier is very similar to that of 19.0 kcal/mol for the process **2** \rightarrow **3**. The route to a second elimination of the OH radical consists of two main steps, rearrangement and radical induced elimination. In the first step, a H-rearrangement from the NH group to the O radical (**6** \rightarrow **7**) proceeds through a four-membered ring transition state with an energy barrier of 30.5 kcal/mol. This energy barrier is higher than the migration of H from $\bullet\text{NH}_2$ to O radical calculated for the **3** to **4** step. The reason for the proposed **6** \rightarrow **7** step followed by **7** \rightarrow **8** is that this sequence provides a plausible way of making the $\text{N}=\text{C}(\text{NH}_2)$ synthon in melamine.

The precursor **8** is a neutral species and is the primary intermediate required for the formation of the cyclic framework in melamine. A H abstraction from **8** by $\bullet\text{NH}_2$ proceeds without an energy barrier to give **9** (Figure 2). The cyclization step **8** \rightarrow **9** proceeds through a relatively low energy barrier of 18.5 kcal/mol. Related cyclization steps have previously been reported as high as 58.3 kcal/mol.²⁰ Again, the second $\text{N}=\text{C}(\text{NH}_2)$ synthon in melamine is formed by the two steps used for **6** \rightarrow **7** \rightarrow **8**, namely, H-rearrangement and radical induced elimination of the OH radical. Similar to the **6** \rightarrow **7** \rightarrow **8** sequence, Figure 2 shows that the H-rearrangement step **10** \rightarrow **11** is characterized by a relatively higher energy barrier than the elimination step **11** \rightarrow **12**. The structure of **12** is a tautomer of melamine. The free radical formation of **12** may take place in the gas phase, or in ice at very low temperature. On the other hand, the tautomerization can take place when **12** gets into an aqueous media in the presence of a base. However, a short sequence of two steps can be used to show that conversion of **12** to melamine can take place via free radical mechanism. A H-abstraction from **12** \rightarrow **13** is barrierless and

exergonic (Table 1). Excluding the ZPE did not affect the energy calculation of the transition state for the step **12** \rightarrow **13**. In this case, **14** which is the resonance structure of **13**, abstracts a H from NH_3 to give melamine **15**. The sequence from **12** to **15** can be regarded as the radical equivalent of the base-catalyzed enol-keto tautomerization; note that the $\bullet\text{NH}_2/\text{NH}_3$ in step **12** \rightarrow **13** is regenerated in step **14** \rightarrow **15**.

3. Mechanisms for the Formation of Ammeline (**22**)

The mechanism in Scheme 2 starts from the neutral intermediate **8** that is formed from either urea or guanylurea. This establishes guanylurea as a precursor for ammeline (**22**). The sequence of steps is similar to that used for the production of melamine. The difference is in the way the radical $\bullet\text{NH}_2$ reacts with **8**. If H abstraction by $\bullet\text{NH}_2$ takes place from the H of H_2N next to $\text{C}=\text{N}$ or $\text{C}=\text{O}$ then the sequence proceeds through the melamine (**15**, Scheme 1) or ammeline (**22**, Scheme 1), respectively.

Figure 3 shows that a H-abstraction from **8** giving **16** occurs without an energy barrier. The cyclization step **16** \rightarrow **17** has a low activation energy of 9.2 kcal/mol. Similar to melamine, the $\text{N}=\text{C}(\text{NH}_2)$ synthon in ammeline is made in a sequence of two steps, namely H-rearrangement followed by elimination. A primary difference from melamine is that the H-rearrangement step takes place from the ring NH to NH radical (**17** \rightarrow **18**). The barrier for this step of 31.5 kcal/mol is similar to that for **6** \rightarrow **7** corresponding to the migration of H to an O radical. Radical induced elimination of $\bullet\text{NH}_2$ leading to a radical molecule complex **19**. A H-abstraction by $\bullet\text{NH}_2$ within the complex **19** yields **20** with a relatively small energy barrier (Figure 3). Ammeline (**22**) is obtained from **21** which is a

resonance structure of **20**. Here, a major difference from melamine mechanisms lies in the presence of radical-molecule complex **19**. In principle, the mechanistic route found for melamine can be adapted in this case as well and vice versa.

4. Mechanism for the Formation of Ammelide (**33**)

The formation of ammelide (**33**) starts from the radical **4** (Scheme 3). Loss of an $\bullet\text{NH}_2$ from **4** is barrierless (Figure 4) and gives the neutral species **23**. Similar to melamine, the barrier for the addition of **2** to the carbonyl group of **23** is 20.3 kcal/mol (Figures 2 and 4). Again, the formation of $\text{N}=\text{C}(\text{NH}_2)$ synthon proceeds through a two-step sequence of 1,3-H rearrangement (**24** \rightarrow **25**) and elimination of $\bullet\text{OH}$ (**25** \rightarrow **26**). This is the same sequence of steps used for the melamine pathway (**3** \rightarrow **4** \rightarrow **5**) in Scheme 1.

The reaction of $\bullet\text{NH}_2$ with the neutral **26** leads to the formation of **27** followed by a cyclization to **28** with an energy barrier of 24.3 kcal/mol. The formation of the second $\text{N}=\text{C}(\text{NH}_2)$ synthon required for the ammelide proceeds through a radical molecule complex **30** that is similar to the sequence of steps for ammeline. Formation of ammelide from **30** is barrierless through **32**. Figure 4 shows a transition state connecting **30** to the low energy structure of **31**; excluding the ZPE from the energy calculations, a small barrier of 1.0 kcal/mol is calculated for step **30** \rightarrow **31**.

5. Mechanism for the Formation of Cyanuric Acid (**39**)

The mechanism for the formation of cyanuric acid (**39**) is distinct from all other triazines because the sequence of steps does not require H-rearrangement steps (Scheme 4). Also, formation of cyanuric acid (**39**) is the shortest mechanism of the triazines. The first step of the mechanism, elimination of $\bullet\text{NH}_2$ from **3** to give biuret **34**, is exergonic

(Table 1) and has a low energy barrier of 9.0 kcal/mol (Figure 5). Addition of **2** to **34** completes the number of C atoms required for cyanuric acid **39**. Elimination of a second $\bullet\text{NH}_2$ in this pathway leads to **36**. This elimination proceeds through a small energy barrier of 2.1 kcal/mol. Note that **36** is symmetric and a hydrogen abstraction using $\bullet\text{NH}_2$ is barrierless and can take place at either end of the molecule. Cyclization of **37** gives **38** with an energy barrier of 10.7 kcal/mol. The final step is the elimination of the third $\bullet\text{NH}_2$ along the route to the formation of the keto tautomer of cyanuric acid **39**.

6. Formation Triazines under Thermal Reactions from Urea

Production of the triazines by heating urea is a well-established process. Large scale production of melamine and biuret has been done by thermal treatment of urea.²⁶ The product distribution for the thermal reactions is quite similar to prebiotic simulation reactions performed in ice/urea. Heating biuret at temperatures of more than 190° C leads to cyanuric acid, ammelide, and ammeline, but melamine was not produced.²⁷ The mechanisms proposed here do predict biuret as a precursor of cyanuric acid (Scheme 4) and are consistent with the fact that melamine was not obtained as a product when biuret was heated. Since biuret does not have a C=NH group, it cannot be a precursor for melamine. In fact, the current mechanism shows that biuret does not lead to intermediate **9** (Scheme 1) that is required for the formation of melamine. Using the proposed approaches, formation of both ammeline and ammelide can be predicted from biuret. Future studies of prebiotic reactions similar to these thermal reactions will enhance understanding of reaction selectivity and product distribution.⁶

7. Keto-Enol Tautomerization of Cyanuric Acid

Formation of the more stable tautomer of an enolizable carbonyl is important in reactions taking place in solution. Cyanuric acid tautomers have been shown to be dependent on pH. Absorption spectra of cyanuric acid are pH dependent. Cyanuric acid adopts the keto form **39** in acid solution.²⁸ Gas phase basicity of cyanuric acid examined by both mass spectrometry and density functional theory at B3LYP/6-31G(d) level of theory suggested that the lowest energy structure of cyanuric acid is the keto tautomer.²⁹ Scheme 4 predicts the formation of the keto-tautomer of cyanuric acid. An advantage of the free radical pathways is the fact that it predicts the appearance of the more stable keto tautomer without pH dependent mechanisms. Tautomerization of the keto-form of cyanuric acid to the enol-form requires a base in a multistep reaction sequence to give the enol-form with aromatic stability; therefore, a possible prebiotic scenario is the conversion of the keto-form of cyanuric acid to the enol-form when it enters in an aqueous media in the presence of a base. The formation of cyanuric acid as well as the other triazines possible in a non-aqueous environment, and the mechanisms suggest that the triazines observed in meteorites may also originate from non-terrestrial and non-aqueous sources.

8. Prebiotic Implications of the Proposed Mechanisms

Because prebiotic systems are dynamic and speculative, the prebiotic events complicate the prediction of the expected products from reactions. The computed DFT results show that urea can form a mixture of products in a non-aqueous environment.

Formation of a mixture of products under less stringent conditions makes these reactions more feasible for prebiotic conditions.

Lack of sufficient information on types, rates, and extent of the prebiotic reactions makes it even more difficult to make a quantitative estimate of the products. Also, previous studies of other biomolecules such as nucleobases have been shown to give low yield of products.³⁰ Experiments have shown that urea is a good precursor for making high yield products of triazines under thermal conditions.²⁶ High yield reactions are prebiotically important and are desired to show accumulation of biomolecules. High energy impact event scenarios that generate a large amount of heat may prove to be important for prebiotic routes for the production of triazines with high yield. Indeed the availability of large amounts of triazines further supports the hypothesis that triazines may have been involved in self-assembly processes.⁹ Since there is no solvent and chemical reagent requirement for the pathways, the proposed reactions are appropriate for the formation of triazines that may contribute to the haze observed in the atmosphere of Titan and most likely on its surface.

IV. Concluding remarks

Using Scheme 1, the main steps of the radical mechanisms can be summarized as follows:

- (a) activation of neutral species (**1**→**2**, **8**→**9**, and **12**→**13**),
- (b) radical attack at carbonyl (**2**→**3**, **5**→**6**, and **9**→**10**),

(c) H-radical intramolecular rearrangement (**3** \rightarrow **4**, **6** \rightarrow **7**, and **11** \rightarrow **12**),

(d) radical induced elimination (**4** \rightarrow **5**, and **11** \rightarrow **12**) and

(e) H-abstraction (**14** \rightarrow **15**).

These types of reactions are used for the formation of all triazines (**22**, **33**, and **39**). It appears that there is a synthetic pattern and logic that is consistent in the mechanisms. For example, formation of the N=C(NH₂) synthon in triazines in all mechanisms are unified in two-step sequence of 1,3-H-rearrangement followed by an elimination step. The keto-form of cyanuric acid is formed and requires the smallest number of steps. On the other hand, the transition states for **20** \rightarrow **22** and **31** \rightarrow **33** are lower in energy than the product because the reactants in these steps have a better resonance stabilization of the free radical site than the free radical in the product (\bullet NH₂); as expected, the transition state has a structure that is slightly at lower energy than the product. Finally, the most important conclusion of the proposed mechanisms is the prediction that biuret is a precursor of cyanuric acid, and guanylurea is a precursor for both melamine and ammeline.

Acknowledgments. The computational work was in part performed at the University of Wisconsin-Madison using Phoenix cluster supported by National Science Foundation Grant CHE-0840494 (NSF, USA). A. Pope and Y. A. Jeilani acknowledge support from the ASPIRE program (Advancing Spelman's Participation in Informatics Research and Education). M. T. Nguyen thanks KU Leuven Research Council for supporting IDO program (IDO) on Exoplanets. C. Pirim and T. M. Orlando also acknowledge support

from the NASA NAI on “Titan as a Pre-biotic Chemical System” at the Jet Propulsion Laboratory.

Supplementary Information. A file contains the Cartesian coordinates of the structures reported and the shape of some radical-neutral complexes.

References

1. S. Derenne, C. Coelho, C. Anquetil, C. Szopa, A. S. Rahman, P. F. McMillan, F. Corà, C. J. Pickard, E. Quirico and C. Bonhomme, *Icarus*, 2012, **221**, 844-853.
2. R. Hayatsu, M. H. Studier, S. Matsuoka and E. Anders, *Geochim. Cosmochim. Acta*, 1972, **36**, 555-571.
3. E. Anders, R. Hayatsu and M. H. Studier, *Origins Life*, 1974, **5**, 57-67.
4. R. Hayatsu, M. H. Studier, L. P. Moore and E. Anders, *Geochim. Cosmochim. Acta*, 1975, **39**, 471-488.
5. R. Hayatsu, M. H. Studier, A. Oda, K. Fuse and E. Anders, *Geochim. Cosmochim. Acta*, 1968, **32**, 175-190.
6. C. Menor-Salvan, D. M. Ruiz-Bermejo, M. I. Guzman, S. Osuna-Esteban and S. Veintemillas-Verdaguer, *Chem. Eur. J.*, 2009, **15**, 4411-4418.
7. R. Briggs, G. Ertem, J. P. Ferris, J. M. Greenberg, P. M. McCain, C. X. Mendoza-Gomez and W. Schutte, *Origins Life Evol. Biospheres*, 1992, **22**, 287-307.
8. I. M. Lagoja and P. Herdewijn, *Chem. Biodiversity*, 2007, **4**, 818-822.
9. B. J. Cafferty, I. Gállego, M. C. Chen, K. I. Farley, R. Eritja and N. V. Hud, *J. Am. Chem. Soc.*, 2013, **135**, 2447-2450.
10. B. R. T. Simoneit, A. Rushdi and D. W. Deamer, *Adv. Space Res.*, 2007, **40**, 1649-1656.
11. S. J. Makowski, M. Lacher, C. Lerner and W. Schnick, *J. Mol. Struct.*, 2012, **1013**, 19-25.
12. D. E. Budil, J. L. Roebber, S. A. Liebman and C. N. Matthews, *Astrobiology*, 2003, **3**, 323-329.
13. M. P. Bernstein, S. A. Sandford, L. J. Allamandola, S. Chang and M. A. Scharberg, *Astrophys. J.*, 1995, **454**, 327-344.
14. Y. A. Jeilani, H. T. Nguyen, D. Newallo, J.-M. Dimandja and M. T. Nguyen, *Phys. Chem. Chem. Phys.*, 2013, **15**, 21084-21093.
15. Y. A. Jeilani, H. T. Nguyen, B. H. Cardelino and M. T. Nguyen, *Chem. Phys. Lett.*, 2014, **598**, 58-64.
16. M. J. Frisch, G. W. Trucks, H. B. Schlegel, G. E. Scuseria, M. A. Robb, J. R. Cheeseman, G. Scalmani, V. Barone, B. Mennucci, G. A. Petersson, H. Nakatsuji,

- M. Caricato, X. Li and H. P. Hratchian, *et al.*, *Gaussian 09, Revision D.01*, Gaussian, Inc., Wallingford CT, 2009.
17. D. Becke, *Phys. Rev. A* 1988, **38**, 3098-3100.
 18. C. Lee, W. Yang and R. G. Parr, *Phys. Rev. B*, 1988, **37**, 785-789.
 19. W. J. Hehre, L. Radom, P. V. R. Schleyer and J. A. Pople, *ab Initio molecular orbital theory*, Wiley, 1986.
 20. J. Wang, J. Gu, M. T. Nguyen, G. Springsteen and J. Leszczynski, *J. Phys. Chem. B*, 2013, **117**, 2314-2320.
 21. J. Wang, J. Gu, M. T. Nguyen, G. Springsteen and J. Leszczynski, *J. Phys. Chem. B*, 2013, **117**, 9333-9342.
 22. G. M. Jensen, D. B. Goodin and S. W. Bunte, *J. Phys. Chem. A*, 1996, **100**, 954-959.
 23. T. Brinck, M. Haeberlein and M. Jonsson, *J. Am. Chem. Soc.*, 1997, **119**, 4239-4244.
 24. Y.-W. Huang, V. Srinivasadesikan, W.-H. Chen and S.-L. Lee, *Chem. Phys. Lett.*, 2013, **565**, 18-21.
 25. C. Menor-Salvan and M. R. Marin-Yaseli, *Chem. Eur. J.*, 2013, **19**, 6488-6497.
 26. B. Bann and S. A. Miller, *Chem. Rev.*, 1958, **58**, 131-172.
 27. P. M. Schabera, J. Colson, S. Higgins, D. Thielen, B. Anspach and J. Brauer, *Thermochim. Acta*, 2004, **424**, 131-142.
 28. I. M. Klotz and T. Askounis, *J. Am. Chem. Soc.*, 1947, **69**, 801-803.
 29. S. Mukherjee and J. Jianhua Ren, *J. Am. Soc. Mass Spectrom.*, 2010, **21**, 1720-1729.
 30. H. L. Barks, R. Buckley, G. A. Grieves, E. Di Mauro, N. V. Hud and T. M. Orlando, *ChemBioChem*, 2010, **11**, 1240-1243.

Table 1.Change in Energies for Prebiotic Formation of Triazines

Reactions	ΔE (kcal/mol)	Reactions	ΔE (kcal/mol)
1 \rightarrow 2	-0.3	21 \rightarrow 22	-3.1
2 \rightarrow 3	13.9	4 \rightarrow 23	14.1
3 \rightarrow 4	0.0	23 \rightarrow 24	3.2
4 \rightarrow 5	25.8	24 \rightarrow 25	2.7
5 \rightarrow 6	1.8	25 \rightarrow 26	2.4
6 \rightarrow 7	2.6	26 \rightarrow 27	9.3
7 \rightarrow 8	0.6	27 \rightarrow 28	1.7
8 \rightarrow 9	9.6	28 \rightarrow 29	5.3
9 \rightarrow 10	14.4	29 \rightarrow 30	0.2
10 \rightarrow 11	-4.0	30 \rightarrow 31	-8.2
11 \rightarrow 12	7.0	32 \rightarrow 33	-4.7
12 \rightarrow 13	-17.1	3 \rightarrow 34	-16.1
14 \rightarrow 15	-1.5	34 \rightarrow 35	20.6
8 \rightarrow 16	20.4	35 \rightarrow 36	-4.2
16 \rightarrow 17	-5.0	36 \rightarrow 37	0.0
17 \rightarrow 18	0.9	37 \rightarrow 38	1.3
18 \rightarrow 19	-5.1	38 \rightarrow 39	-11.8
19 \rightarrow 20	-8.2		

Legends for Figures and Schemes

Figure 1. Structures of the selected triazines

Figure 2. Potential energy profile for formation of melamine (**15**). The profile represents the relative potential energies of a sequence of reactions. Relative energy is the zero-point energy corrected relative energy. Color representation for atoms are: white for H, grey for C, blue for N, and red for O.

Figure 3. Potential energy profile for formation of ammeline (**22**). The profile represents the relative potential energies of a sequence of reactions. Relative energy is the zero-point energy corrected relative energy. Color representation for atoms are: white for H, grey for C, blue for N, and red for O.

Figure 4. Potential energy profile for formation of ammeline (**33**). The profile represents the relative potential energies of a sequence of reactions. Relative energy is the zero-point energy corrected relative energy. Color representation for atoms are: white for H, grey for C, blue for N, and red for O.

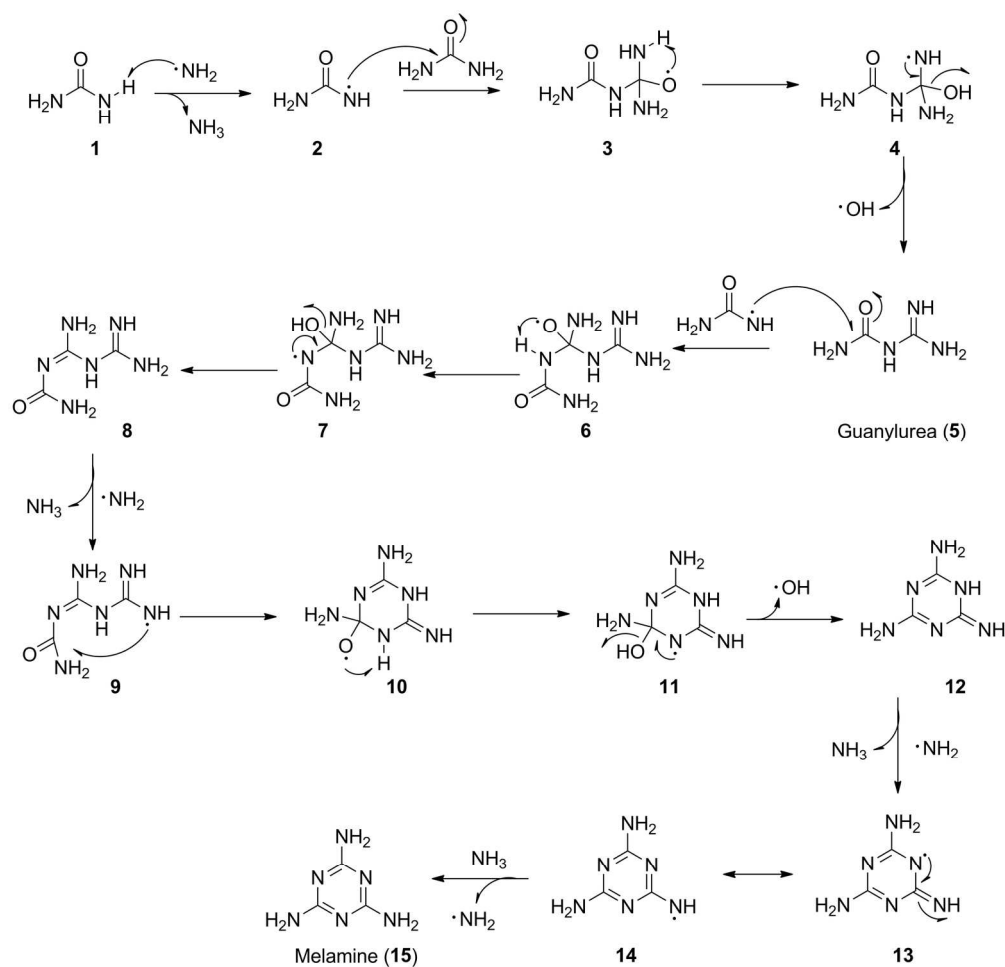
Figure 5. Potential energy profile for formation of cyanuric acid (**39**). The profile represents the relative potential energies of a sequence of reactions. Relative energy is the zero-point energy corrected relative energy. Color representation for atoms are: white for H, grey for C, blue for N, and red for O.

Scheme 1. Mechanisms for formation of melamine (**15**)

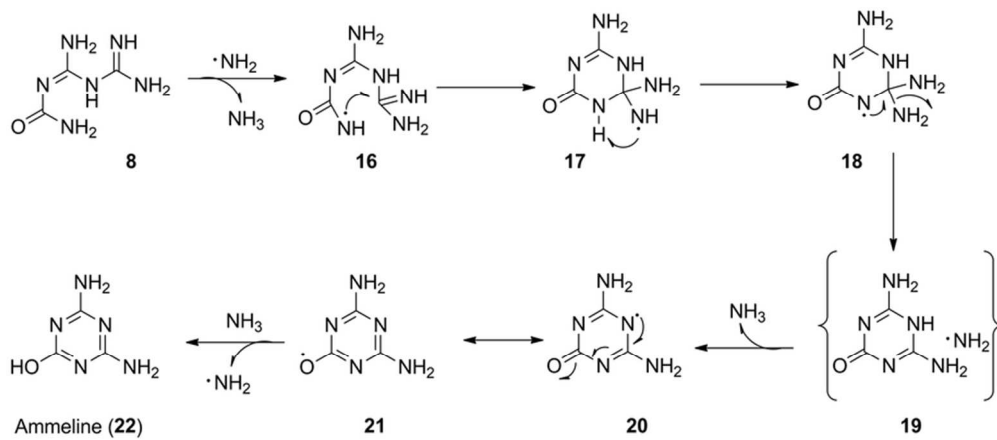
Scheme 2. Mechanisms for formation of ammeline (**22**)

Scheme 3. Mechanisms for formation of ammeline (**33**)

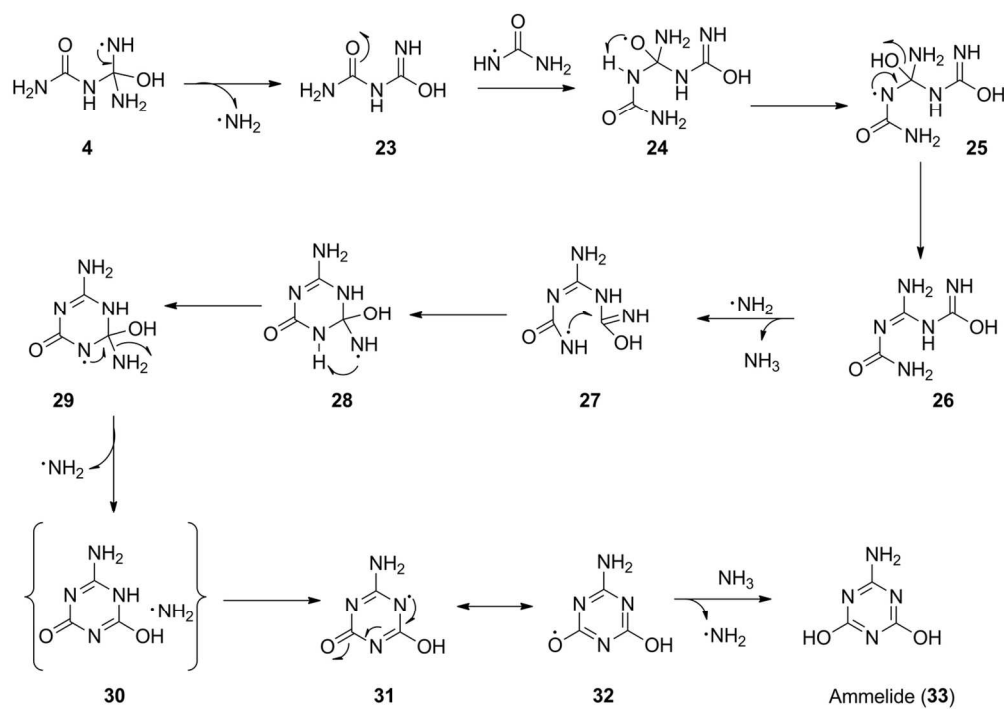
Scheme 4. Mechanisms for formation of cyanuric acid (**39**)



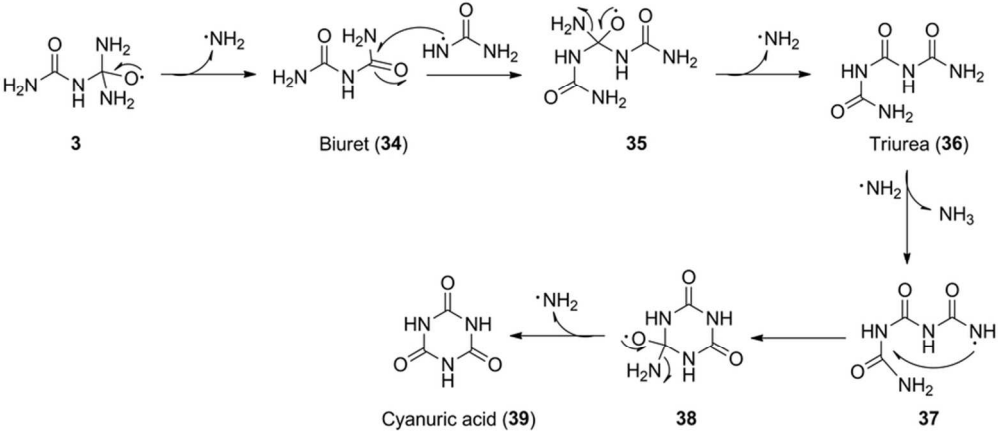
Scheme 1. Mechanisms for formation of melamine (15)
175x167mm (300 x 300 DPI)



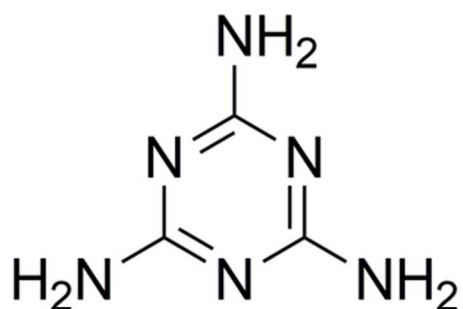
Scheme 2. Mechanisms for formation of ammeline (22)
77x33mm (300 x 300 DPI)



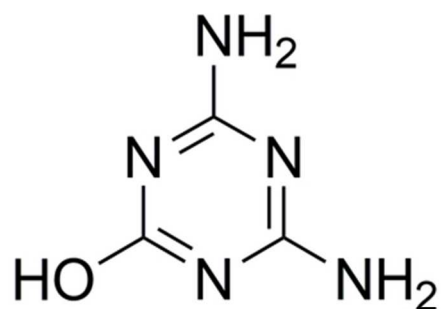
Scheme 3. Mechanisms for formation of ammelide (33)
127x89mm (300 x 300 DPI)



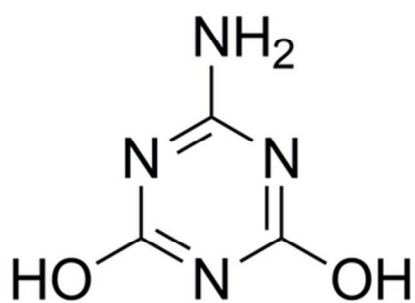
Scheme 4. Mechanisms for formation of cyanuric acid (39)
80x35mm (300 x 300 DPI)



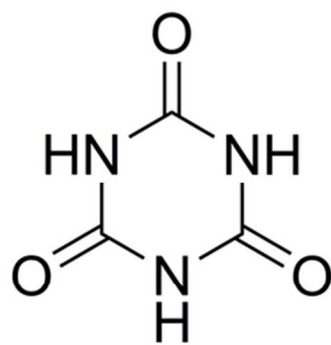
Melamine



Ammeline



Ammelide



Cyanuric acid

Figure 1: Structures of the selected triazines
63x63mm (300 x 300 DPI)

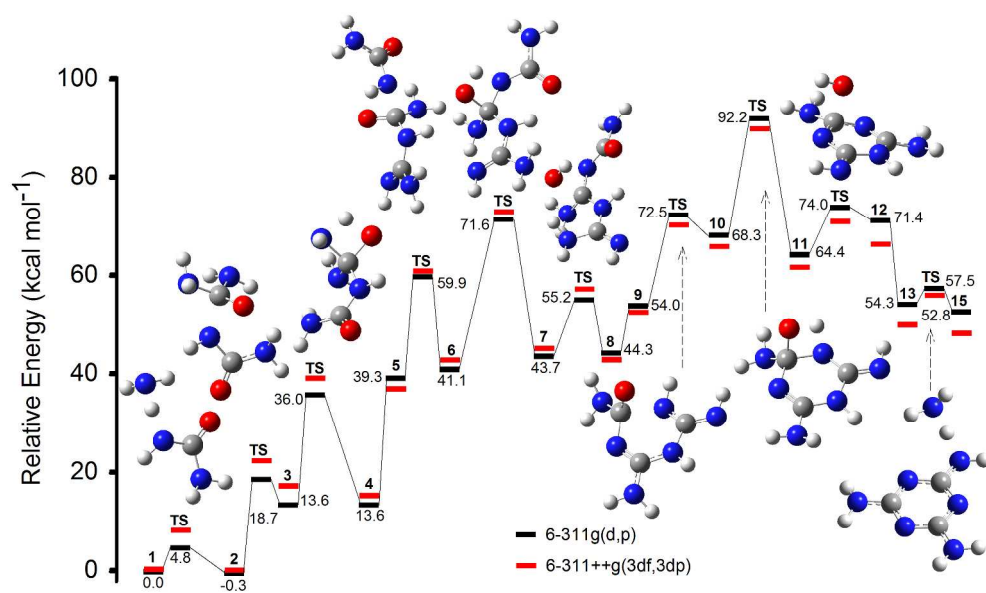


Figure 2. Potential energy profile for formation of melamine (15). The profile represents the relative potential energies of a sequence of reactions. Relative energy is the zero-point energy corrected relative energy. Color representation for atoms are: white for H, grey for C, blue for N, and red for O
281x172mm (300 x 300 DPI)

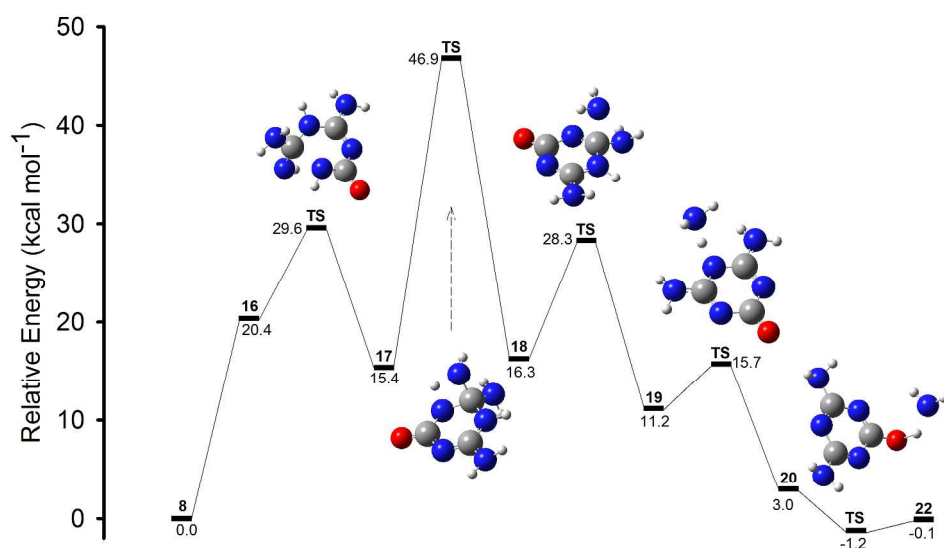


Figure 3. Potential energy profile for formation of ammeline (22). The profile represents the relative potential energies of a sequence of reactions. Relative energy is the zero-point energy corrected relative energy. Color representation for atoms are: white for H, grey for C, blue for N, and red for O.
276x166mm (300 x 300 DPI)

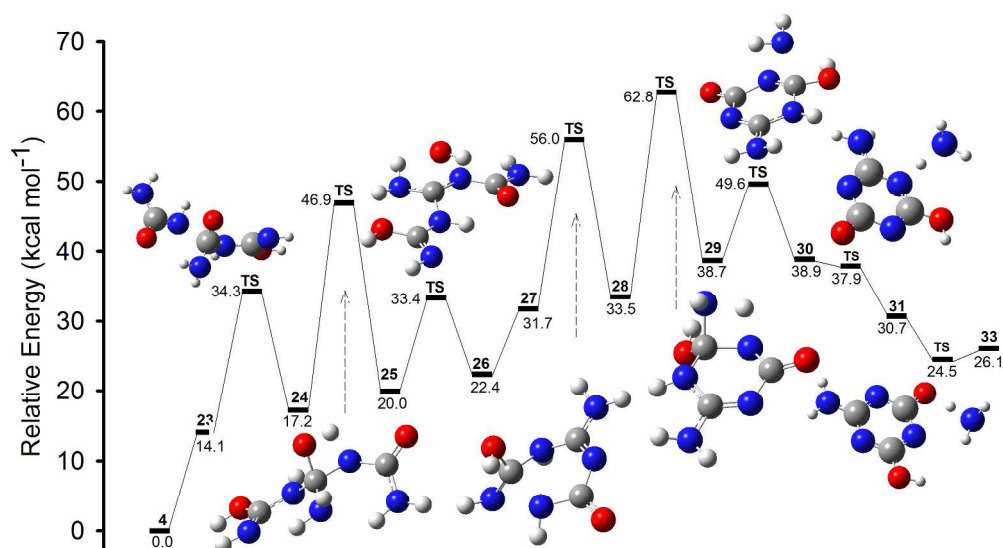


Figure 4. Potential energy profile for formation of ammelide (33). The profile represents the relative potential energies of a sequence of reactions. Relative energy is the zero-point energy corrected relative energy. Color representation for atoms are: white for H, grey for C, blue for N, and red for O.
276x166mm (300 x 300 DPI)

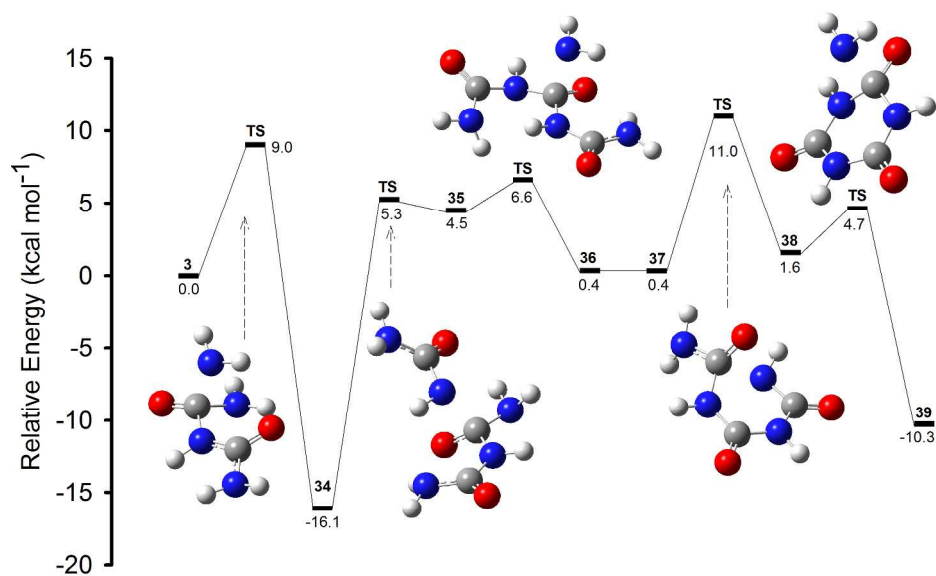


Figure 5. Potential energy profile for formation of cyanuric acid (39). The profile represents the relative potential energies of a sequence of reactions. Relative energy is the zero-point energy corrected relative energy. Color representation for atoms are: white for H, grey for C, blue for N, and red for O.

278x166mm (300 x 300 DPI)